JACS
JOURNAL OF THE AMERICAN CHEMICAL SOCIETY

COMMUNICATION

pubs.acs.org/JACS

Synthesis, Crystal Structure, and Physical Properties of Sterically Unprotected Hydrocarbon Radicals

Takashi Kubo,*[,†] Yoshiki Katada,[†] Akihiro Shimizu,[†] Yasukazu Hirao,*[,†] Kazunobu Sato,[‡] Takeji Takui,[‡] Mikio Uruichi,[§] Kyuya Yakushi,[§] and Robert C. Haddon*[,∥]

[†]Department of Chemistry, Graduate School of Science, Osaka University, Toyonaka, Osaka 560-0043, Japan

[‡]Department of Chemistry, Graduate School of Science, Osaka City University, Sumiyoshi-ku, Osaka 558-8585, Japan

[§]Institute of Molecular Science, Myodaiji, Okazaki, Aichi 444-8585, Japan

[∥]Departments of Chemistry and Chemical and Environmental Engineering, University of California, Riverside, California 92521, United States

Supporting Information

ABSTRACT: We have prepared and isolated neutral polycyclic hydrocarbon radicals. A butyl-substituted radical gave single crystals, in which a π-dimeric structure, not a σ-bonded dimer, was observed, even though steric protection was absent. Thermodynamic stabilization due to the highly spin-delocalized structure contributes effectively to the suppression of σ-bond formation.

Organic radicals have long fascinated chemists with a fundamental understanding of structure−reactivity relationship in organic reactions[1] and with applications for electroconductive[2] and magnetic materials.[3] Although most radicals are chemically reactive species and are encountered only as intermediates, some are stable enough to be isolated even in air.[4] When one considers the use of radicals as building blocks for materials, kinetic and thermodynamic stabilizations are essential for a long life. Kinetic stabilization, which is usually steric protection, leads to interference of the orbital interaction between radicals and consequently suppresses σ-bond formation but, at the same time, is undesirable for electroconductive and magnetic properties. Thus thermodynamic stabilization is key to the development of functional materials based on organic radicals.

Unlike heteroatom-centered radicals, which are well studied in terms of the functionality,[3] hydrocarbon radicals have been far from application due to a strong propensity for σ-dimerization originating from the strength of the carbon−carbon bond.[5] All the hydrocarbon radicals isolated so far in a crystalline form take advantage of kinetic stabilization (**1**−**6**, Chart 1).[6] In this context, we decided to explore the preparation of hydrocarbon radicals that are stabilized predominantly by a thermodynamic factor. In this paper, we show that a large extent of spin delocalization is effective for suppressing σ-dimerization of hydrocarbon radicals.

Our molecular design is strongly based on the high spin-delocalizing nature of phenalenyl radical.[7] An unpaired electron of this radical delocalizes over six equivalent carbon atoms due to its symmetry,[8] as shown in Figure 1. This highly spin-delocalized structure leads to the thermodynamic stability of this radical, which is inferred from the fact that the bond dissociation energy of the methylene C−H bond in phenalene is one of the weakest among closed-shell hydrocarbons (270 kJ mol^{-1}).[9] However, the phenalenyl radical is in equilibrium with a σ-dimer in solution,[10] and consequently, steric protection (see, **6**)[6f] or attachment of heteroatoms[11] is required for isolating it in a radical form in the solid state.

The compound **7** is the radical that we newly designed (Figure 2). This radical is composed of two phenalenyl rings, and an unpaired electron can delocalize over the whole molecule through the resonance of two canonical forms having a phenalenyl radical structure (Figure 2a).[12] Within the framework of the Hückel molecular orbital (HMO) theory, the singly occupied molecular orbital (SOMO) of **7** is distributed on 12 carbon atoms, and its coefficients are $\pm 1/\sqrt{12}$, that is, the spin density on the phenalenyl ring of **7** is half of those of the phenalenyl radical (Figure 2b). Thus **7** is more thermodynamically stabilized than the phenalenyl radical.

Scheme 1 shows the synthetic route for **7**. The starting material, 6-bromophenalanol **8**, was prepared according to the literature.[13] Reduction of the hydroxyl group with Et_3SiH and subsequent coupling of the lithiated **9** with ethyl formate gave bis-phenalanyl methanol **10**. Cyclization with H_3PO_4 and dehydrogenation with dichlorodicyano-*p*-benzoquinone (DDQ) gave a cationic species of **7**. This cationic species was not suitable for measuring cyclic voltammetry because of the presence of the DDQ counteranion, and therefore we replaced the DDQ anion with tetrafluoroborate (**14**). The target radical **7** was obtained as a black powder by the reduction of **14** with decamethylferrocene.

A toluene solution of **7** gave a very well-resolved multiline electron spin resonance (ESR) spectrum at room temperature. However, the complex pattern made it difficult to determine the proton hyperfine coupling constants (a_H) by computer simulation. Therefore we applied the ENDOR/TRIPLE technique for the most reliable a_H values. The technique can afford both the magnitudes and relative signs for a_H's. Figure 3 shows the observed (sideband production free) and simulated ESR spectra of **7** along with the a_H values (the ^{1}H ENDOR/TRIPLE spectra are shown in Figure S1, Supporting Information). The agreement between the experimental and theoretical a_H values (Figure 3c) indicates that the delocalization of the unpaired electron is not confined to one phenalenyl ring but is operative over the entire molecule. The intensity of the ESR signal remained unchanged even at −90 °C, indicative of no dimerization process upon cooling. This result contrasts markedly with the behavior of parent

Received: July 14, 2011
Published: August 11, 2011

ACS Publications © 2011 American Chemical Society

Chart 1. Hydrocarbon Radicals Isolated so Far in a Crystalline form

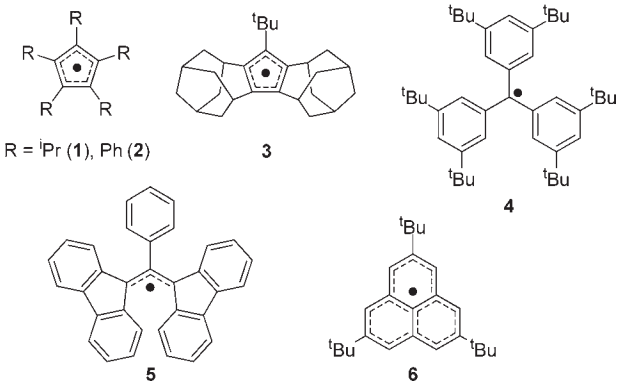

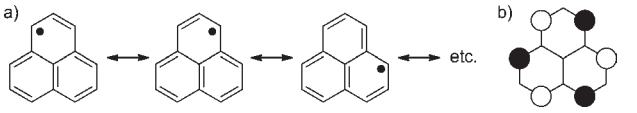

Figure 1. (a) Spin delocalization of phenalenyl radical. Each canonical form contributes equally to the ground state. (b) The SOMO of phenalenyl radical. The SOMO coefficients are $\pm 1/\sqrt{6}$ at the 6 equivalent carbons and 0 at the remaining 7 in terms of the HMO approximation.

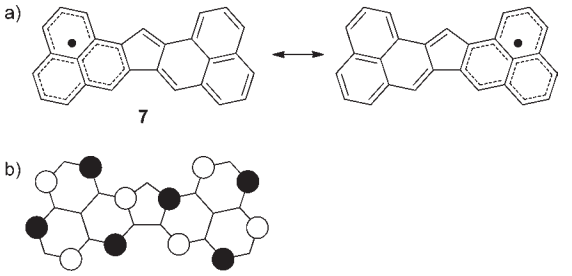

Figure 2. (a) Spin delocalization of the newly designed radical **7**. (b) The SOMO of **7** by the HMO calculation. The SOMO coefficients are $\pm 1/\sqrt{12}$ at the positions corresponding to the 6 equivalent carbons of phenalenyl radical and 0 at the remaining 15 in terms of the HMO approximation.

phenalenyl radical and 2,5,8-tri-*tert*-butlylphenalenyl radical **6**, whose ESR signal intensities drastically decrease upon cooling due to σ-[14] and π-dimerization,[15] respectively.

Cyclic voltammogram of **14** in CH_2Cl_2 gave two reversible redox waves at -0.39 and -1.42 V vs Fc/Fc^+ (Figure S2, Supporting Information). The difference between the first (cation to radical) and the second (radical to anion) reduction potentials is 1.03 V, which corresponds to the disproportionation potential (ΔE) of **7**. The ΔE of **7** is much smaller than that of phenalenyl radical (1.6 V),[16] indicative of a larger thermodynamic stability of **7**. As mentioned above, neutral radicals are good potential candidates for single component molecular conductors, in which a small on-site Coulomb repulsion (U) is one of the essential factors.[17] The U can be estimated from ΔE of neutral radicals. The ΔE of **7** is still large for the application to organic metals, because the bandwidth (W) of most organic solids is less than 0.5 eV and a higher ratio of W/U, especially $W > U$, is required for metallic behavior.[17]

Scheme 1. Synthetic Route for 7 and 16[a]

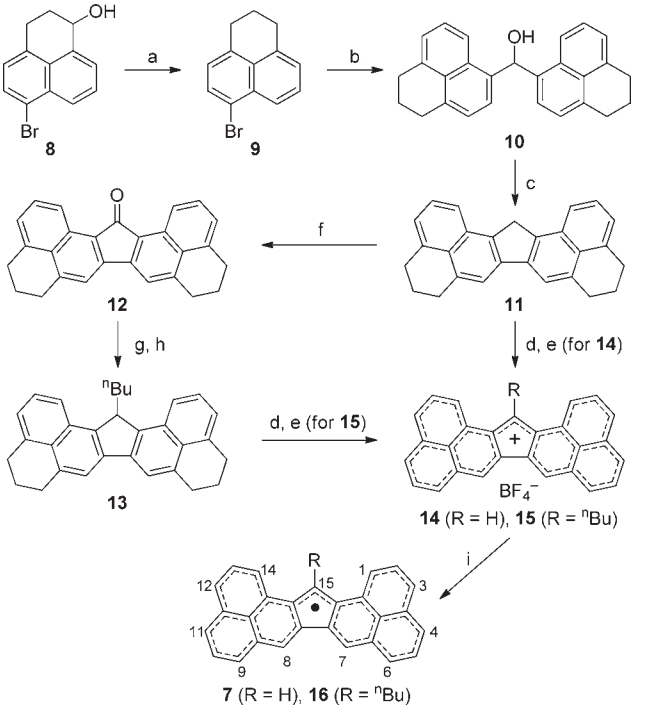

[a] Reagents and conditions: (a) Et_3SiH, TFA, CH_2Cl_2, rt, 88%; (b) ^{n}BuLi, then HCO_2Et, ether, -30 to 0 °C, 88%; (c) H_3PO_4, 180 °C, 24%; (d) DDQ, toluene, 70 °C; (e) $^n Bu_4NBF_4$, TFA, rt, 83% for **14** (2 steps) and 41% for **15** (2 steps); (f) Triton-B, air, pyridine, rt, 63%; (g) ^{n}BuLi, THF, rt; (h) Et_3SiH, TFA, CH_2Cl_2, rt, 78% (2 steps); and (i) decamethylferrocene, CH_2Cl_2, trifluoroacetic acid (TFA).

Further characterization, including single crystal X-ray diffraction analysis, could not be carried out due to the low solubility of **7** in most organic solvents. Therefore we decided to introduce a butyl group that is distantly positioned from the phenalenyl rings, in order to increase the solubility.

The butyl-substituted radical **16** was prepared as shown in Scheme 1. A butyl group was introduced by the attack of butyl anion to the ketone group in **12**. Dehydrogenation of **13** with DDQ and a subsequent exchange of counteranions gave a cationic species as a tetrafluoroborate salt (**15**). The radical **16** was obtained as black needles by the reduction of **15** with decamethylferrocene in a sealed degassed tube.

Our primary interest for **16** is the absence of σ-bond formation between radicals in the solid state. As shown in Figure 4, **16** formed a π-dimer, not a σ-dimer, in which many C−C contacts that are shorter than the sum of the van der Waals radius of carbon atom were observed. Some of the carbon atoms bearing α-(positive) spin density, which correspond to the active carbons of phenalenyl radical, participate in the short contacts. The very short contacts suggest a bonding interaction of two unpaired electrons in the π-dimer. Such a multipoint bonding interaction of unpaired electrons is referred to as multicenter bonding,[18] which has attracted attention as a new type of chemical bond. The attractive force within the π-dimer originates from a covalent bonding interaction due to a large SOMO−SOMO overlap as well as from a conventional dispersion force between π-planes. On the other hand, there is no short contact of α-spin-bearing carbons between the π-dimers, and therefore a dominant interdimer interaction is a dispersion force.

dx.doi.org/10.1021/ja2065768 |J. Am. Chem. Soc. 2011, 133, 14240–14243

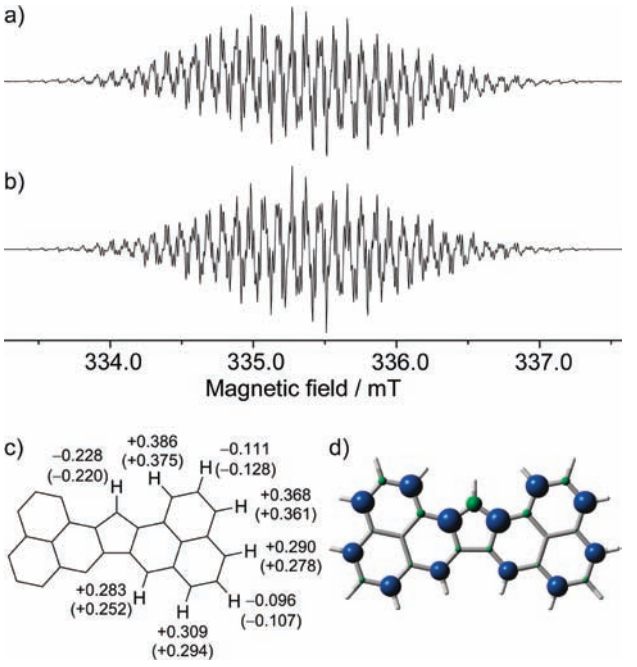

Figure 3. (a) Observed (8.18×10^{-4} M, $g = 2.0027$, $\nu = 9.509400$ GHz, at room temperature) and (b) simulated ESR spectra of **7**. (c) The a_H values determined. In parentheses, the a_H values calculated with a UBLYP/6-31G**//UB3LYP/6-31G** method are also shown. (d) Spin density map calculated with a UBLYP/6-31G**//UB3LYP/6-31G** method. Blue and green surfaces represent α and β spin densities drawn at 0.004 e/au^3 level, respectively.

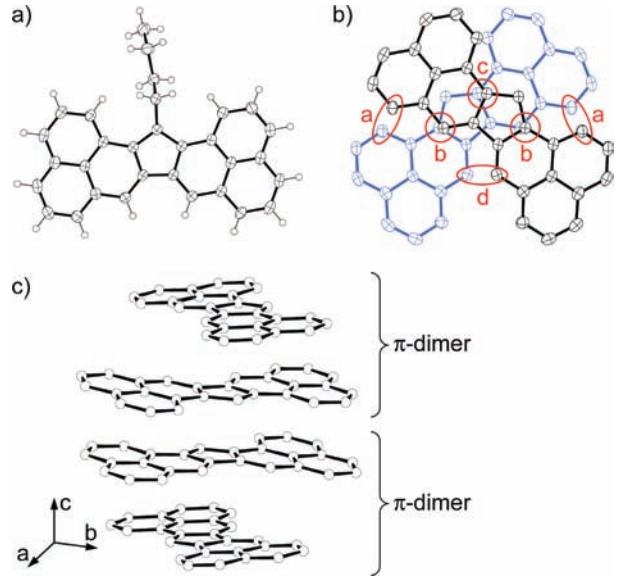

Figure 4. (a) The ORTEP drawing of **16** with thermal ellipsoids at 50% probability. (b) Top view of the π-dimer of **16**. Butyl groups and hydrogen atoms are omitted for clarity. Red ellipses indicate the short contacts of carbon atoms that possess α-spin density. The C−C distances in Å are: a, 3.383; b, 3.138; c, 3.341; and d, 3.096. (c) Molecular stacking along *c*-axis.

The strength of the covalent bonding interaction within the π-dimer was estimated by SQUID measurements (Figure S3, Supporting Information). The measurement showed an increasing susceptibility above 220 K. Careful fitting of the observed

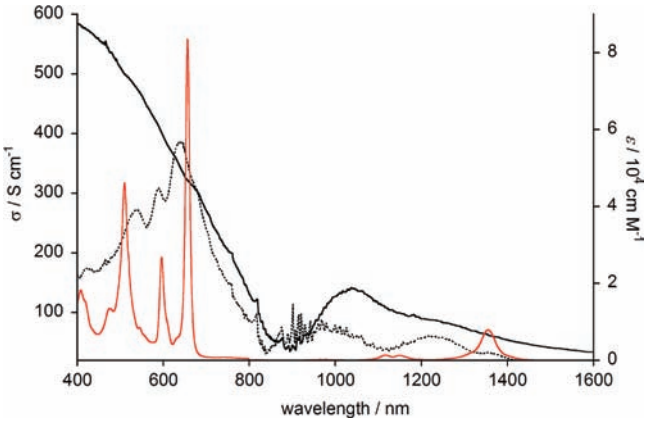

Figure 5. Optical spectra of **16**. Absorbance (ε) in toluene (red line) and optical conductivities (σ) obtained with light polarized along (black solid line) and perpendicular to the *c*-axis (black dotted line) on the single crystal (3 −1 0) face.

increase using the Bleaney−Bowers equation[19,20] in a single-t−triplet model indicates the antiferromagnetic coupling ($2J/k_B$) of almost −1600 K within the π-dimer.

The relatively large antiferromagnetic coupling would split the SOMO of **16** into bonding and antibonding molecular orbitals within the π-dimer. A polarized reflection spectrum of a single crystal of **16** gave a band at 1037 nm along the *c*-axis ($E//c$), as shown in Figure 5. This band is not observed in a reflection spectrum obtained with light polarized perpendicular to the *c*-axis ($E\perp c$) and in a solution spectrum. The band observed along the *c*-axis is assignable to the transition from highest occupied molecular orbital (HOMO) to lowest unoccupied molecular orbital (LUMO) of the π-dimer. A time-dependent (TD) RB3LYP/6-31G* calculation of the π-dimer predicts a partially allowed HOMO−LUMO band at 1110 nm ($f = 0.14$) along the line connecting the two molecules, thoroughly supporting the assignment.

The longest-wavelength absorption band (1355 nm, ε = 7910 cm M^{-1}) in a toluene solution of **16** is assigned to a transition from SOMO to LUMO, according to a TD-UB3LYP/6-31G** calculation of **7** that predicts a weak band at 1143 nm ($f = 0.06$). From the decay of this near IR band, we estimated the stability of **16** in the solution state open to air in the dark. The half-life determined at room temperature was almost 60 h, which is in contrast to the rapid reaction of phenalenyl radical with oxygen.[21]

Finally, we discuss the thermodynamic stability of **7** from a theoretical point of view. Thermodynamic stability of neutral radicals ($R^\bullet$) can be estimated by a radical stabilization energy (RSE) that is evaluated with a second-order restricted open-shell Møller−Plesset theory (ROMP2) calculation for isodesmic hydrogen-transfer reactions defined as eq 1.[22] We calculated the

$$CH_3^\bullet + R-H \xrightarrow{\Delta H(=\mathrm{RSE})} CH_4 + R^\bullet \qquad (1)$$

RSE of allyl radical, phenalenyl radical, and **7** at the ROMP2/6-31G**//UB3LYP/6-31G** level of theory. The calculated RSEs (in kJ mol^{-1}) were 78.11 for the allyl and 201.64 for the phenalenyl radicals and 209.23 for **7**. The RSE of phenalenyl radical is extraordinarily large compared to that of allyl radical. This is an interesting finding because the RSE of fluorenyl radical, which has the same number of sp^2-carbon atoms as the phenalenyl radical, was only 92.99 kJ mol^{-1} at the same level of calculation. While the difference of the RSE between phenalenyl radical and **7** is only

7.59 kJ mol^{-1}, **7** has a larger RSE than the phenalenyl radical. However, this slight advantage in thermodynamic stability indeed leads to suppressing a σ-bond formation. According to the study by Kochi and co-workers,[10] phenalenyl radical stands on a delicate balance between σ- and π-dimerizations (the bond enthalpies for the σ and π-dimer are 42 and 40 kJ mol^{-1}, respectively). This means that an electronic perturbation on phenalenyl radical could tilt the balance in favor of π-dimerization. The preference of π-dimerization found in the dithiophenalenyl radical, which is stabilized by electronic effects of heteroatoms,[11] is the representative case. In the case of **7**, the delocalization of an unpaired electron on one phenalenyl ring into the other phenalenyl ring contributes to the further stabilization.

In summary, we have succeeded in isolating a hydrocarbon radical in a crystalline form, without the use of steric protection. The large extent of spin delocalization suppressed σ-bond formation between the radicals. In the solid state, the radical formed a π-dimer, in which unpaired electrons covalently interacted through multicenter bonding. The antiferromagnetic coupling amounted to almost −1600 K, and this relatively large coupling split the SOMO of the radical into bonding and antibonding molecular orbitals.

Polycyclic hydrocarbon radicals with the RSE larger than that of phenalenyl radical might remain discrete in the solid state, and the search for new stable hydrocarbon radicals will open up new avenues for electroconductive and magnetic materials. The work is currently in progress in our laboratories.

■ ASSOCIATED CONTENT

Supporting Information. Experimental procedure for all new compounds; crystal data; ^{1}H ENDOR/TRIPLE spectra; cyclic voltammogram; magnetic susceptibility plot; details on the theoretical calculations; and CIF file of **16**. This material is available free of charge via the Internet at http://pubs.acs.org.

■ AUTHOR INFORMATION

Corresponding Author
kubo@chem.sci.osaka-u.ac.jp; y-hirao@chem.sci.osaka-u.ac.jp; haddon@ucr.edu

■ ACKNOWLEDGMENT

The authors are grateful to Dr. Arindam Sarkar, Dr. Leanne Beer, and Dr. Puhong Liao for useful discussions. This work was supported in part by the Office of Basic Energy Sciences, Department of Energy, under grant DE-FG02-04ER46138 (R.H.), Yamada Science Foundation (T.K.), the Grants-in-Aid for Scientific Research on Innovative Areas "Organic Synthesis Based on Reaction Integration, Development of New Methods, and Creation of New Substances" (no. 2105, T.K.), KAKENHI (no. 22750129, Y.H.), and "Quantum Cybernetics" (no. 2112004, T.T.), CREST-JST (T.T.), and FIRST-JSPS (Quantum Information Process, T.T.).

■ REFERENCES

(1) Fossey, J.; Lefort, D.; Sorba, J. *Free Radicals in Organic Chemistry*; Wiley: New York, 1997; pp 1−322.
(2) (a) Haddon, R. C. *Aust. J. Chem.* **1975**, *28*, 2343–2351. (b) Haddon, R. C. *Nature* **1975**, *256*, 394–396.
(3) *Magnetic Properties of Organic Materials*; Lathi, P. M., Ed.; Marcel Dekker: New York, 1999; pp 1−728.
(4) (a) Hicks, R. G. *Org. Biomol. Chem.* **2007**, *5*, 1321–1338.(b) *Stable Radicals: Fundamental and Applied Aspects of Odd-electron Compounds*; Hicks, R., Ed.; Wiley-Blackwell: New York, 2010; pp 1−606.
(5) Griller, D.; Ingold, K. U. *Acc. Chem. Res.* **1976**, *9*, 13–19.
(6) (a) Sitzmann, H.; Boese, R. *Angew. Chem., Int. Ed. Engl.* **1991**, *30*, 971–973. (b) Janiak, C.; Weimann, R.; Görlitz, F. *Organometallics* **1997**, *16*, 4933–4936. (c) Kitagawa, T.; Ogawa, K.; Komatsu, K. *J. Am. Chem. Soc.* **2004**, *126*, 9930–9931. (d) Kahr, B.; Engen, D. V.; Gopalant, P. *Chem. Mater.* **1993**, *5*, 729–732. (e) Azuma, N.; Ozawa, T.; Yamauchi, J. *Bull. Chem. Soc. Jpn.* **1994**, *67*, 31–38. (f) Goto, K.; Kubo, T.; Yamamoto, K.; Nakasuji, K.; Sato, K.; Shiomi, D.; Takui, T.; Kubota, M.; Kobayashi, T.; Yakusi, K.; Ouyang, J. *J. Am. Chem. Soc.* **1999**, *121*, 1619–1620.
(7) (a) Reid, D. H. *Q. Rev.* **1965**, *19*, 274–302.(b) For a recent review: Morita, Y.; Nishida, S. In *Stable Radicals: Fundamental and Applied Aspects of Odd-electron Compounds*; Hicks, R., Ed.; Wiley-Blackwell: New York, 2010; Chapter 3.
(8) Nishida, S.; Kariyazono, K.; Yamanaka, A.; Fukui, K.; Sato, K.; Takui, T.; Nakasuji, K.; Morita, Y. *Chem.—Asian J.* **2011**, *6*, 1188–1196.
(9) (a) Bausch, M. J.; Gostowski, R.; Jirka, G.; Selmarten, D.; Winter, G. *J. Org. Chem.* **1990**, *55*, 5805. (b) Gerst, M.; Rüchardt, C. *Chem. Ber.* **1993**, *126*, 1039–1045.
(10) Zaitsev, V.; Rosokha, S. V.; Head-Gordon, M.; Kochi, J. K. *J. Org. Chem.* **2006**, *71*, 520–526.
(11) Beer, L.; Mandal, S. K.; Reed, R. D.; Oakley, R. T.; Tham, F. S.; Donnadieu, B.; Haddon, R. C. *Cryst. Growth Des.* **2007**, *7*, 802–809.
(12) The idea of canonical resonance to stabilize radicals has been successfully employed in heterocyclic radicals. See: Beer, L.; Brusso, J. L.; Cordes, A. W.; Haddon, R. C.; Itkis, M. E.; Kirschbaum, K.; MacGregor, D. S.; Oakley, R. T.; Pinkerton, A. A.; Reed, R. W. *J. Am. Chem. Soc.* **2002**, *124*, 9498–9509.
(13) Boekelheide, V.; Goldman, M. *J. Am. Chem. Soc.* **1954**, *76*, 604–605.
(14) Gerson, F. *Helv. Chim. Acta* **1966**, *49*, 1463–1467.
(15) Small, D.; Zaitsev, V.; Jung, Y.; Rosokha, S. V.; Head-Gordon, M.; Kochi, J. K. *J. Am. Chem. Soc.* **2004**, *126*, 13850–13858.
(16) Haddon, R. C.; Wudl, F.; Kaplan, M. L.; Marshall, J. H.; Cais, R. E.; Bramwell, F. B. *J. Am. Chem. Soc.* **1978**, *100*, 7629–7633.
(17) (a) Garito, A. F.; Heeger, A. *J. Acc. Chem. Res.* **1974**, *7*, 232–240. (b) Torrance, J. B. *Acc. Chem. Res.* **1979**, *12*, 79–86.
(18) (a) Suzuki, S.; Morita, Y.; Fukui, K.; Sato, K.; Shiomi, D.; Takui, T.; Nakasuji, K. *J. Am. Chem. Soc.* **2006**, *128*, 2530–2531. (b) Mota, F; Miller, J. S.; Novoa, J. J. *J. Am. Chem. Soc.* **2009**, *131*, 7699–7707. (c) Tian, Y. -H.; Huang, J.; Kertesz, M. *Phys. Chem. Chem. Phys.* **2010**, *12*, 5084–5093. (d) Tian, Y. -H.; Kertesz, M. *J. Am. Chem. Soc.* **2010**, *132*, 10648–10649.
(19) Bleaney, B.; Bowers, K. D. *Proc. R. Soc. London, Ser. A* **1952**, *214*, 451–465.
(20) The spin−spin interaction between the π-dimer would be very small because the amount of singlet biradical character in the dimeric pair between the π-dimers amounts to 90%, following the natural orbital analysis based on a broken-symmetry UB3LYP/6-31G* calculation. Therefore we used the singlet−triplet model, not the antiferromagnetic 1D Heisenberg chain model, for the analysis of the SQUID data.
(21) Reid, D. H. *Tetrahedron* **1958**, *3*, 339–352.
(22) (a) Zipse, H. *Top. Curr. Chem.* **2006**, *263*, 163–189. (b) Hioe, J.; Zipse, H. *Org. Biomol. Chem.* **2010**, *8*, 3609–3617.